

The subsurface observation of fault-zone trapped waves: applications to investigations of the deep structure of active faults

Takashi Mizuno*

Disaster Prevention Research Institute, Kyoto University

Abstract

Analyzing fault-zone trapped waves is an effective approach to imaging the deep structure of fault zones. In this paper, we apply a fault-zone trapped wave analysis to investigate the deep structure of the Nojima and the Mozumi-Sukenobu faults in Japan. We observed fault-zone trapped waves at subsurface seismic stations. We obtained typical candidates of fault-zone trapped waves at subsurface stations. The duration of fault-zone trapped waves becomes larger with hypocenter distance. This result indicates that trapped waves were generated at the hypocenter and traveled along the fault zone. We then estimated the averaged fault zone structure from hypocenter to receiver. The thickness and the shear wave velocity of the fault zone were estimated by fitting synthetic dispersion curves and waveforms to the observed ones. The thickness of the fault zone is estimated to be 150–290 m for the Nojima fault and 130–400 m for the Mozumi-Sukenobu Fault. For both of these fault-zones, the shear-wave velocity is reduced by 10 to 20% of the surrounding velocity. The low-velocity fault zones of the Nojima and the Mozumi-Sukenobu faults continue to a depth of about 10 km from the locations of the earthquakes showing trapped waves. For the Nojima fault, the thickness and the shear-wave velocity of the fault zone are not comparable with those estimated from previous surface observations. This discrepancy might be due to distortions of the seismograms caused by surface observations and lateral variations of fault-zone structure. The trapped waves tend to be degraded by thick sediments near the surface. Borehole observations will be required to detect typical fault-zone trapped waves, and enable us to analyze fault-zone property with high accuracy.

Key words: deep structure of fault zone, trapped wave, subsurface observation

1. Introduction

The nature of the fault zone structure is a key factor in investigating the dynamics of faulting. During the faulting processes, stored elastic energy is released as radiated elastic waves and heat, and also is consumed in the formation of the fault zone structure. Geological (e.g., Chester *et al.*, 1993; Tanaka *et al.*, 2001) and rock mechanical (e.g., Scholz *et al.*, 1993; Vermilye and Scholz, 1998) studies have revealed that the fault zone comprises many kinds of fault rocks formed over history by the faulting. Some studies have found relations between fault

zone thickness and cumulative displacements (e.g., Blenkinsop, 1989; Evans, 1990; Shipton and Cowie, 2001). They found that the total thickness of the fault zone increases as the displacement is accumulated. Zhang *et al.* (2000) studied a zone of distributed microcracks (process zone) surrounding the tip of a propagating fracture. They pointed out that the damage zone acts as an inelastic deformation zone at the propagation of the crack tip. Additionally, numerical modeling of damaged-zone formation has been performed using the discrete element method (e.g., Astrom *et al.*, 2000). However, there is a lack of

* e-mail: takashi.mizuno@aist.go.jp (Central 7, Higashi-1-1, Tsukuba, Ibaraki, Japan) Now at Earthquake process research group, Geological Survey of Japan, AIST.

information on the large-scale fault-zone structures of active faults, so the evolution mechanism of faults on a scale of tens to hundreds of kilometers is not well understood.

The other motivation is to discuss whether the fault zone can act as a conduit for fluid. Rock mechanics and seismological studies argue for the importance of fluids supplied from the lower crust in the faulting process (e.g., Sibson, 1992; Byerlee, 1990; Byerlee, 1993; Yamashita, 1998; Maillot *et al.*, 1999; Zhao and Mizuno, 1999; Mizuno *et al.*, 2001). These studies commonly suggest that fluids control the pore pressure and the effective stress applied to the fault plane. The diversity of seismic activity may be controlled by the heterogeneous distribution of fluids within the crust. However, the distribution of crack density and saturation rate is not well known for actual fault zones. To quantify crack density and saturation rate within fault zones, the seismic structure of fault zone is important.

In this paper, we investigate the deep fault zone structure by analyzing fault-zone trapped waves. Geological and geophysical studies suggest that the thickness of the fault-zone of an active fault has a length scale of hundreds of meters (e.g., Chester *et al.*, 1993; Tanaka *et al.*; 2001; Ohtani *et al.* 2001). Conventional methods of reflection and refraction seismology have tried to image the seismic velocity structure in and around the fault zone (e.g., Thurber *et al.*, 1997; Hole *et al.*, 2000; Zhao and Negishi, 1998; Park *et al.*, 2000). However, to image deep fault zone structures on the scale of tens to hundreds of meters, unrealistic station and source densities are required. Therefore, the tomographical study could not infer the fault-zone structure. In reflection seismology, the reflected energy is too weak to image the fault zone structure of steeply dipping faults.

An analysis of the trapped waves has been applied to investigations of low-velocity layered structures such as coal seams (e.g., Rader *et al.*, 1985; Reguero, 1990; Dresen and Ruter, 1994) and subducted slabs (e.g., Hori *et al.*, 1985). The analysis of trapped waves uses the waveform of the shear wave and its following part. Therefore, seismic waveforms with a good signal-to-noise ratio are required to image fault zone structures from an analysis of the fault-zone trapped wave. The fault-zone structure may be obtained more precisely by subsurface obser-

vations than by conventional surface observations. In this paper, we use high-quality waveform data recorded at subsurface stations at the Nojima and the Mozumi-Sukenobu faults, Japan, to estimate the fine seismic structure of these fault zones.

2. Theoretical background, observation and analysis of the fault-zone trapped waves

Cracks and joints are distributed around the fault plane with a high density (Scholz *et al.*, 1993). In the case of wavelengths of the seismic wave are much longer than the scale of each crack, the total elastic property of the medium can be treated as a homogeneous low-velocity zone (e.g., O'Connell and Budiansky, 1974; Hudson 1980). In this case, channel waves that travel within the fault-zone can be expected. Such waves are known as fault-zone trapped waves (e.g., Li *et al.*, 1998; Ben-Zion, 1998) and show the characteristics listed below:

- (1) large amplitude within a fault zone;
- (2) particle motion polarized into the fault-parallel direction;
- (3) propagating along the fault zone;
- (4) normal dispersion;
- (5) dominant frequency that almost corresponds to the frequency showing the minimum phase velocity.

We identify trapped waves from observed seismograms based on the characteristics listed above. Trapped waves can be modeled using several different procedures. The simplest method is to model the dispersion curve of the group velocity. Rader *et al.* (1985) introduced a calculation algorithm for the dispersion and the amplitude of the trapped wave by introducing the complex phase shift of the plane wave reflected at the boundaries of the fault zone. Ben-Zion and Aki (1990) and Ben-Zion (1998) derived an analytical expression of trapped waves in a 2-D medium within a frequency-wavenumber domain. These techniques are only applicable to a 2-D uniform structure, low-velocity layer sandwiched between two half spaces. A finite difference method has also been applied to calculations of fault-zone trapped waves (e.g., Li *et al.*, 2000; Mamada *et al.*, 2002). However, the finite-difference method consumes more time than that of the analytical method. For simplicity, we modeled the fault zone to be a 2-D uniform structure. We then obtained an averaged

fault zone structure from source to receiver using the analytical solution of the group-velocity dispersion curve of Rader (1985) and the synthetic waveform calculation algorithm of Ben-Zion and Aki (1990).

3. Application to active faults in Japan: the Nojima and the Mozumi-Sukenobu faults

3.1 The Nojima fault

The Nojima fault was ruptured at the Kobe earthquake, 1995. The length of the fault is estimated to be 13km from geographical studies (e.g., The research group for active faults in Japan, 1991, Fig. 1 a and Table 1). We used seismograms recorded at the DPRI 1800-m borehole (TOS2), operated by the Disaster Prevention Research Institute, Kyoto University. This station is at the southern end of the Nojima fault. TOS2 is equipped with a three-component seismometer with a natural frequency of 4.5 Hz (Nishigami *et al.*, 2001). From geophysical loggings, TOS2

was considered to be located near the boundary of the fault zone (Nishigami *et al.*, 2001, Fig. 1 b). At the Nojima fault, we did not deploy an array observation in the borehole; therefore, we could not diagnose the characteristics of (1) and (3) listed on section 2. We selected a few specific events using characters of (2), (4) and (5) on section 2. We identified 6 records of

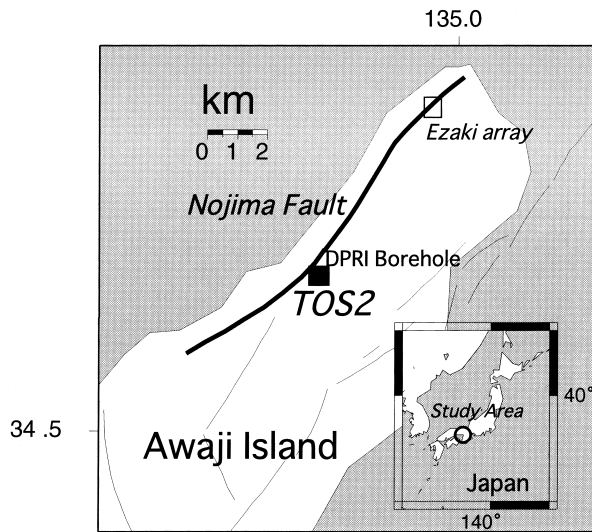


Fig. 1. (a) Map showing station location of TOS2 (■). TOS2 was located at the southern part of the Nojima fault. Ezaki array (□) operated by Li *et al.* (1998) is also shown. Solid line denotes the surface trace of the Nojima fault.

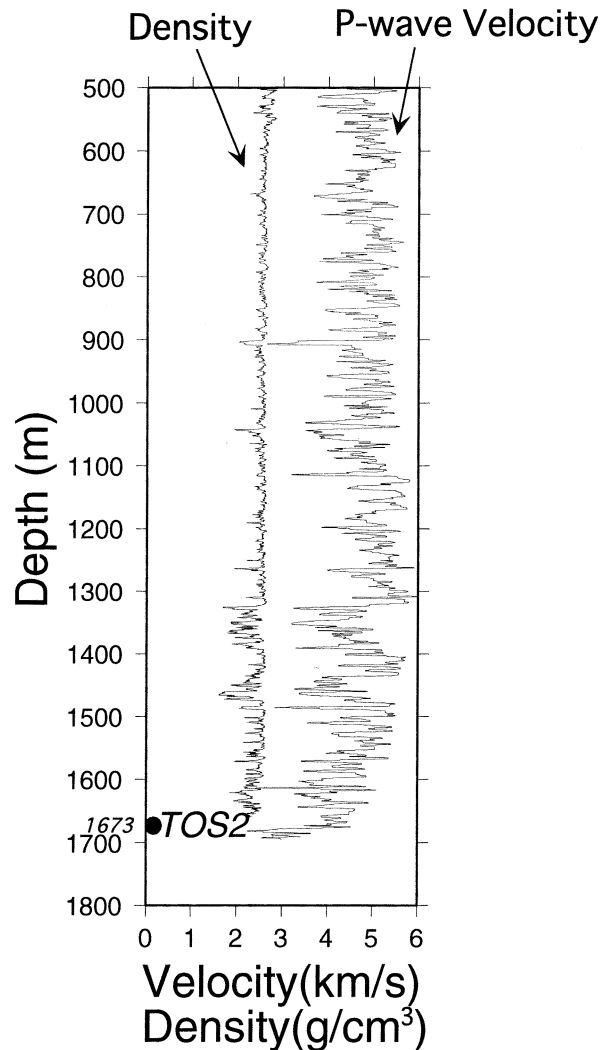


Fig. 1. (b) Geophysical logging in the DPRI 1800 m borehole. Black circle denotes the location of the seismometer.

Table 1. The features and physical properties of two active faults.

	Nojima Fault	Mozumi-Sukenobu Fault
Length (km)	13	23
Displacement (km)	0.5 - 1.1	0.2 - 0.5
Slip type	Strike slip	Strike slip
Latest large event	Kobe Eq. In 1995 (M7.2)	Hietsu Eq. In 1858 (M6.9)
Width of the FZ (m)	150 - 290	130 - 400
S-wave velocity of FZ (km/s)	2.6 - 3.0	2.8 - 3.1
Qs of FZ	40 - 90	60 - 90

fault-zone trapped waves from the seismograms of 465 natural earthquakes occurring in and around the Nojima and Rokko fault system (Fig. 2a). Fig. 3 shows the record section of the trapped waves. We observed that the duration of trapped waves increases with distance. Therefore, we expect that the trapped waves were generated at the source, and traveled along the fault zone. Based on the hypocenter locations of earthquakes showing trapped waves, the Nojima fault appears to dip southeastward at 75 degrees and down to a depth of 10 km (Fig. 2b).

We modeled the dispersion curve and the waveform of trapped waves. As shown in Fig. 3, we can expect that the trapped waves travelled along the fault zone, however, the apparent velocity of trapped waves changes slightly. We observed that the average apparent velocities of trapped waves were 2.6 km/s for shallower events and 3.0 km/s for deeper events (Fig. 3). This result implies that the fault-zone structure has a spatial variation, especially for the velocity structure. Figs 4 and 5 show the observed and synthetic dispersion curve and waveforms, respectively. We sought thickness and shear wave velocity of the fault zone estimated in this study to best explain the observations for each the six events. Details of the analysis are documented in Mizuno and Nishigami (2003). The thickness, shear-wave velocity and Q_s of the fault zone were estimated to be 150 m to 290 m, 2.6 km/s to 3.0 km/s, and 40 to 60, respectively.

Fig. 2b shows an earthquake cluster occurring near the shallow part of the fault zone. The error at the hypocenter location is about 0.5 km in this study (Nagai *et al.*, 2001). Therefore, we could not infer the location of each event with respect to the fault zone only from hypocenter information. In this study, we identified typical trapped waves for one event. Therefore, we can explain that most of the clustering earthquakes did not occur within the fault zone. Observations of trapped waves enable us to locate them with respect to the fault zone with high accuracy.

3.2 The Mozumi-Sukenobu fault

The Mozumi-Sukenobu fault belongs to the Atotsugawa fault system of central Japan (Fig 6). The Mozumi-Sukenobu fault has a strike of N40° E to N60° E and length of 23 km (The research group for active faults in Japan, 1991, Fig. 6 and Table 1). The

cumulative displacement is estimated to be 0.5 km (The research group for active faults in Japan, 1991). The latest earthquake that occurred at the Mozumi-Sukenobu fault is estimated to be the Hietsu earthquake, $M=6.9$ in 1858 (Takeuchi *et al.*, 1999). In addition, the Atotsugawa fault system is located along the Niigata-Kobe tectonic zone, which is recognized as having a high strain rate (Hashimoto and Jackson, 1993; Sagiya *et al.*, 2000). The Atotsugawa fault system is one of the most energetic active faults in Japan.

A 300-m-deep survey galley penetrates the western part of the Mozumi-Sukenobu fault (Ando, 1999). We used seismograms recorded at the seismic array operated at the survey gallery (Fig. 7). Two fault zones have been recognized by the geological survey in the survey gallery (Fig. 7). The seismic array is equipped with 32 three-component seismometers with a natural frequency of 2 Hz, spaced about 15 m apart (Fig. 7), and arranged perpendicularly to the strike of the Mozumi-Sukenobu fault.

We observed nine events showing typical trapped waves for 154 earthquakes that occurred from May 28, 1997 to June 1, 2001 around the Mozumi-Sukenobu fault (Fig 9). Fig. 8 shows examples of candidates of trapped waves. The top of Fig. 8 shows an example of the fault-parallel component of the trapped wave recorded at m208. The bottom of Fig. 8 shows the waveform of the fault-parallel component at all stations. A dispersive wavetrain was observed following the direct shear-wave arrival, especially within the fracture zones A and B. From the locations of earthquakes showing trapped waves, the Mozumi-Sukenobu fault continues down to a depth of at least 11 km, and dips to the south at an angle of about 75 to 85 degrees (Fig. 9). Figs 10 and 11 show the observed and synthetic dispersion curves and waveforms, respectively. Details of the analysis are documented by Mizuno *et al.* (2003). Thickness, shear-wave velocity, and Q_s of the fault zone were estimated to be 160 m to 400 m, 2.9 km/s to 3.1 km/s, and 60 to 90, respectively (Table 1). The width of the fault zone was comparable to the extent of the distribution of fracture zones within the survey gallery.

4. Discussions

4.1 Discrepancy between our results and previous results

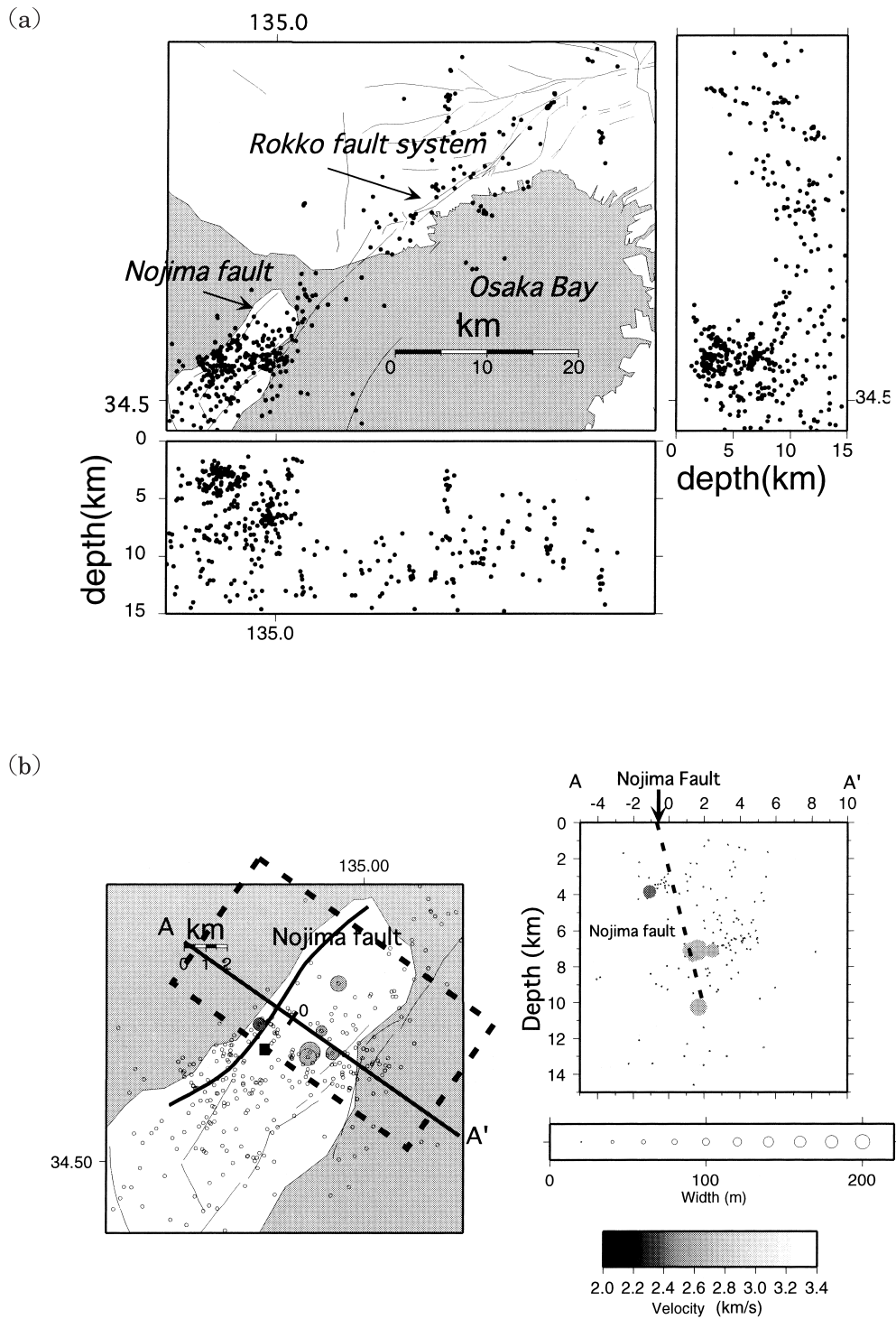


Fig. 2. (a) Hypocenter distribution used in this study (January 1, 1999-May 18, 2000).

(b) The distribution of the hypocenters of events used in this study (small open circle) and with typical trapped waves (solid symbols) are shown. The thickness and the shear wave velocity of the fault zone are expressed by the radius and gray-scale of the circles. (Left) Map showing hypocenter distribution. (Right) Vertical cross-sections of hypocenter distribution along AA' in the left figure. The dotted line indicates the fault plane of the Nojima fault suggested by this study.

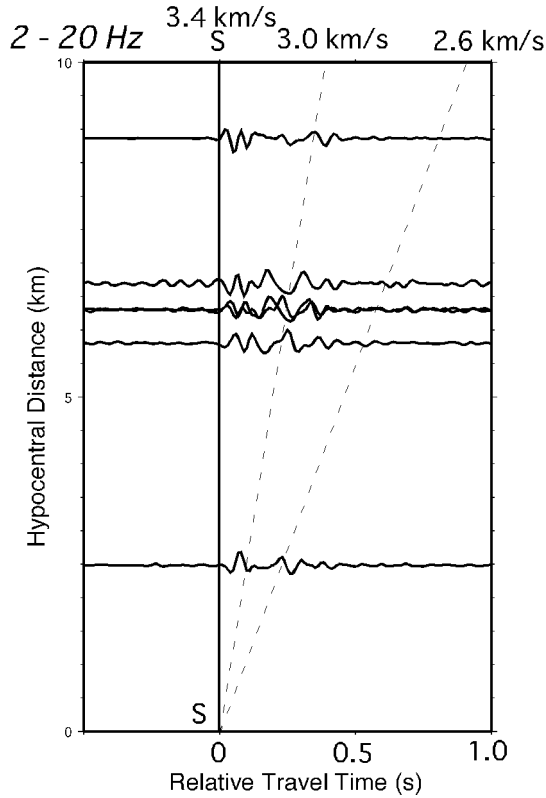


Fig. 3 Paste-up of the fault parallel component of the trapped-waves. The time of shear wave arrival of each waveform was synchronized. The dashed line indicates the arrival time for shear wave velocities of 3.0 (left) and 2.6 km/s (right).

The fault-zone width and shear-wave velocity we obtained were larger than those of previous studies; the width was 20 to 40 m and the shear-wave velocity was 1.0 to 1.8 km/s (e.g., Li *et al.* 1998; Ito and Kuwahara, 2000; Nishigami and Okuma, 1996). Fig. 12a shows examples of trapped waves recorded at the Ezaki array (Fig. 1a) by Li *et al.* (1998). The hypocentral distance is about 8 km, which almost corresponds to our observations (except for 000119.051459). Two arrows in Fig. 12a indicate the arrival time of the direct shear wave and the tail of the trapped wave. From the surface observation, the duration of the trapped waves was about 1 second. However, the duration of trapped waves recorded at the borehole did not exceed 0.5 seconds. The durations of trapped waves recorded at TOS2 were shorter than the trapped waves recorded at the Ezaki array. Fig. 12b represents comparisons between our observation and the synthetic waveform of Li *et al.* (1998) and Nishigami and Okuma (1996). The fit be-

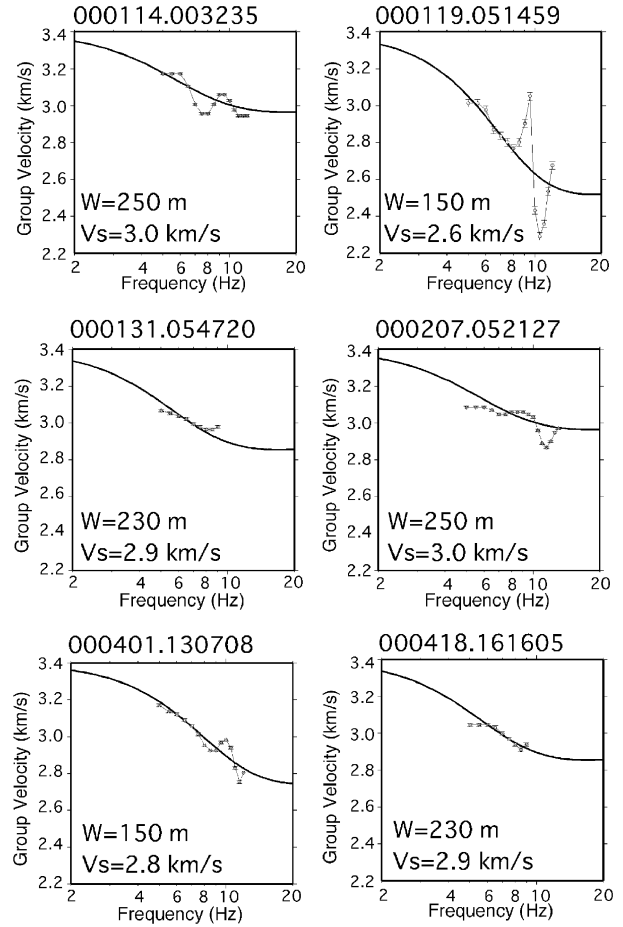


Fig. 4. Observation (thin line) and best-fit model (thick line) of the group velocity dispersion curve (fundamental model) of typical trapped waves. Best fitting model parameters are also shown; W: thickness of the fault zone, Vs: shear-wave velocity of the fault zone.

tween the observation and synthetic waveforms is poor, especially for duration of the trapped waves. Therefore, we consider the wider fault-zone model estimated in this study to be preferable for explaining our observations. There are two possible reasons for the discrepancy. TOS2 is about 7 km from the Ezaki array used by Li *et al.* (1998) (Fig. 1a). Therefore, it is possible that the fault-zone structure has lateral variations. The other reason is the heterogeneous structure near the surface. Murata *et al.* (2001) reported that there is a sedimentary layer about 100–400 m thick on Awaji Island. A wavetrain with a long duration observed at the surface might be composed of trapped waves and other phases such as scattering waves generated near the surface. We cannot conclude the reason for the discrepancy only

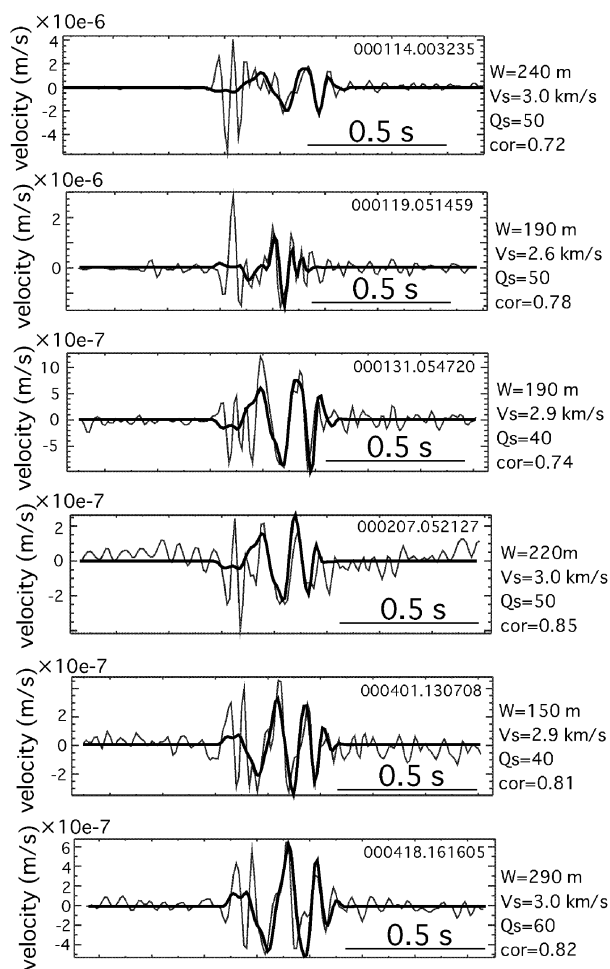


Fig. 5. Observed (thin line) and best-fit synthetic waveforms (thick line). Parameters for each model are denoted at the right side of the figures; Qs: shear-wave attenuation factor of the fault zone.

from this study, however, we can further study the mechanism of the discrepancy between the borehole and the surface observations through dense surface and borehole observations of trapped waves.

There are some reports of temporal changes of properties of seismic structures associated with large earthquakes (e.g., Matsumoto *et al.*, 2000; Baisch and Bokelmann, 2001; Tadokoro *et al.*, 2002). To infer temporal variations of fault zone properties, stable and high accurate observations are preferable. Borehole observations also enable us to infer temporal variations of fault-zone properties without the effects of the shallow structure around the observatory. However, borehole observations are expensive. For the most of the studies on temporal variations of seismic structure, temporal changes were observed from surface observations. Therefore, a combination

of the surface and subsurface observations is realistic.

4.2 Fault zone structure and its evolutionary process

The evolution of a fault progresses over millions or billions of years, so it is not easy to infer the evolution process of an active fault. Vermilye and Scholz (1998) suggested, using observational and theoretical methods, that faults has evolved in association with the repetition of slips. They predict that the width and the length of a fault should be extended in association with evolution. The Mozumi-Sukenobu fault is twice as long as the Nojima fault. Therefore, we assume that the Mozumi-Sukenobu fault has evolved over a longer period than the Nojima fault. We speculate on the process of fault-zone evolution by comparing the fault-zone structures of these two faults, which have different ages.

We estimated the width of the Nojima fault to be about 210 m. The average width of the Mozumi-Sukenobu fault was estimated to be about 280 m, with its fault zone being 1.3 times wider than that of the Nojima fault. The length of each fault was estimated from geographical studies (Research Group for Active Faults in Japan, 1991). Fig. 13 is a diagram of the widths and the lengths of the faults. The widths of the fault zones of the two faults are widely scattered; however, we may suggest that the width of a fault zone might be proportional to the length of a fault. In addition, The widths of the fault zones of the two faults are well explained by the model of Vermilye and Scholz (1998), based on observational studies of the faults using one-to-hundreds meter scales. The fault evolution process may be length-scale invariant. This result may indicate that the evolutionary process of a fault found by the study for the small scale faults is applicable to a discussion of the evolutionary process of a large active fault. To discuss the scaling of the fault zone quantitatively, we should carry out more observational studies of the fault zone in the future.

4.3 Cooperation between trapped wave technique and seismic tomography

In this section, we compare two models of the velocity structure near the fault zone -one obtained by trapped waves and one by seismic tomography. In this study, we estimated that the fault zone was 150 m to 290 m wide, and its velocity 10 to 20% less

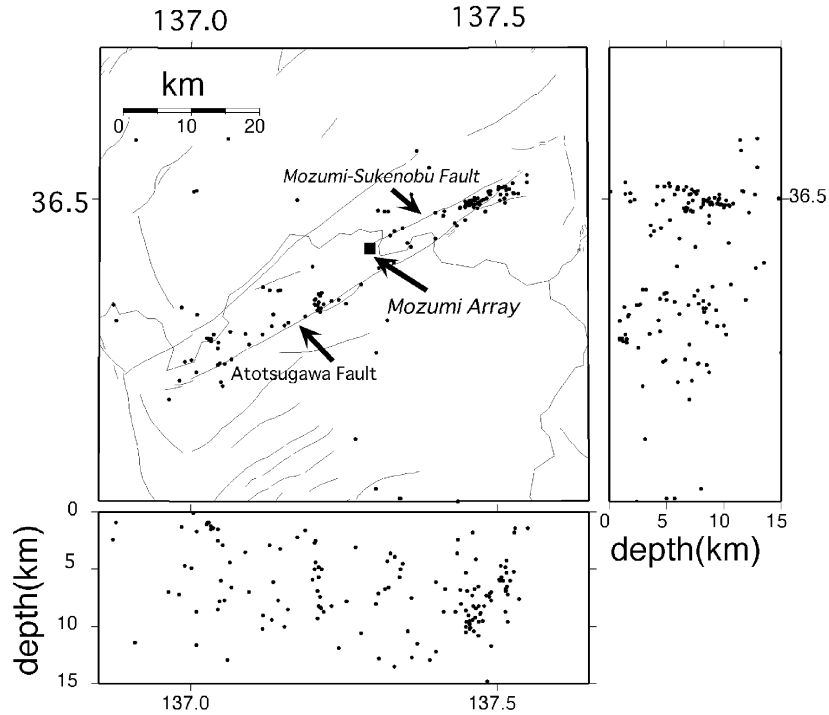


Fig. 6. Hypocenter distribution used in this study (May 28, 1997-June 1, 2001). The location of the observation gallery is also shown (■).

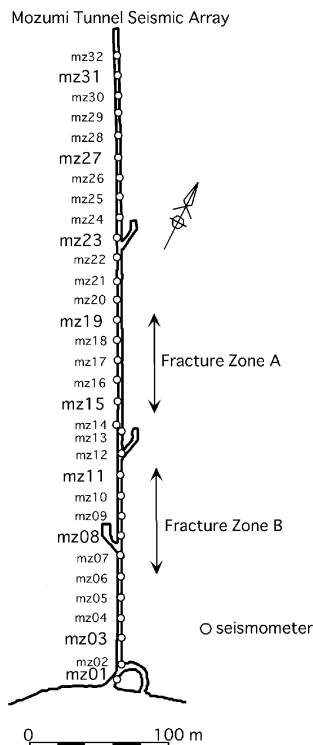


Fig. 7. Distribution of seismometers (circle) and fracture zones (A and B) in the observation tunnel at the Mozumi-Sukenobu fault.

than the surrounding velocity. The Nojima fault seems to continue down to a depth of 10 km. Zhao and Negishi (1998) studied the P and S wave velocity structure in and around the Nojima and Rokko fault system using a seismic tomography technique with a resolution of 5 km. They obtained a low-velocity anomaly of 3 to 6% at the shallow part (to a depth of 10 km) distributed along the surface trace of the Nojima fault. Zhao and Negishi (1998) pointed out that the tomographic method may not infer the fault-zone structure because of the resolution. For the Nojima fault, we conclude that the tomographic image could not clearly resolve the fault-zone structure, especially for the width and shear-wave velocity of fault zones. Obviously, the fault-zone trapped waves could not infer the large-scale velocity structure around the fault zone. To image the detailed velocity structure in and around the fault zone, a combination of trapped waves and tomographic study is required.

The velocity reduction within the fault zone can be associated with a high dense crack distribution. The theoretical study of O'Connell and Budiansky (1974) suggests that velocity reduction is controlled by crack density defined as $\epsilon = n \times a^3$, where n is the number density of cracks, and a is the average radius

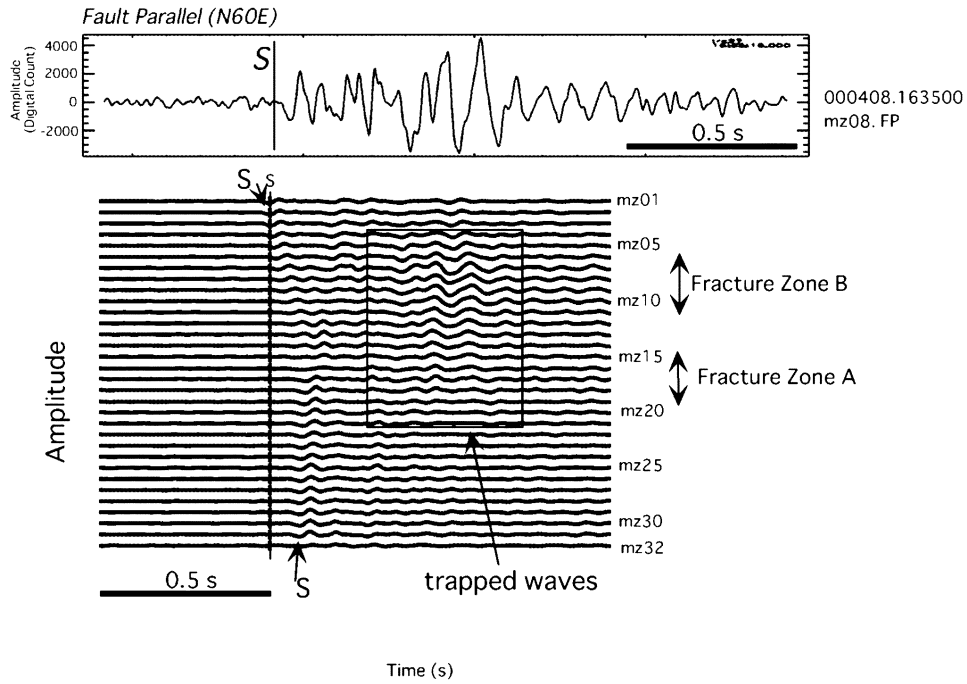


Fig. 8. An example of observations of fault-zone trapped waves. (a) (top) Waveform of the fault-parallel component of a candidate of trapped wave recorded at mz08. (bottom) All of the fault parallel component seismograms of 000408.163500. Waveforms are arranged by the number of the seismometer shown in Fig. 7. Each seismogram is synchronized with the onset of the direct S-wave arrival. The amplitude of each trace is normalized by the maximum amplitude of each trace.

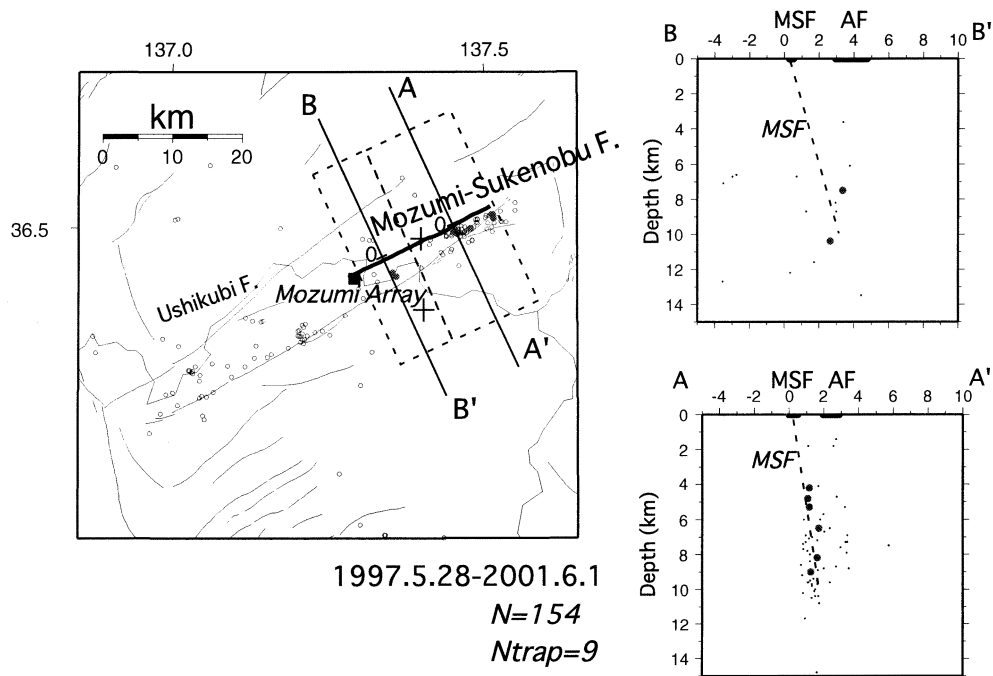


Fig. 9. The open circle expresses the hypocenter used in this study. The solid circle denotes the hypocenter of the earthquake showing trapped waves. (left) Map view of the hypocenter distribution. (right) Vertical cross sections of hypocenter distribution along the lines AA' (top) and BB' (bottom) in the map. Dotted lines indicate the fault plane of the Mozumi-Sukenobu fault that is suggested by this study.

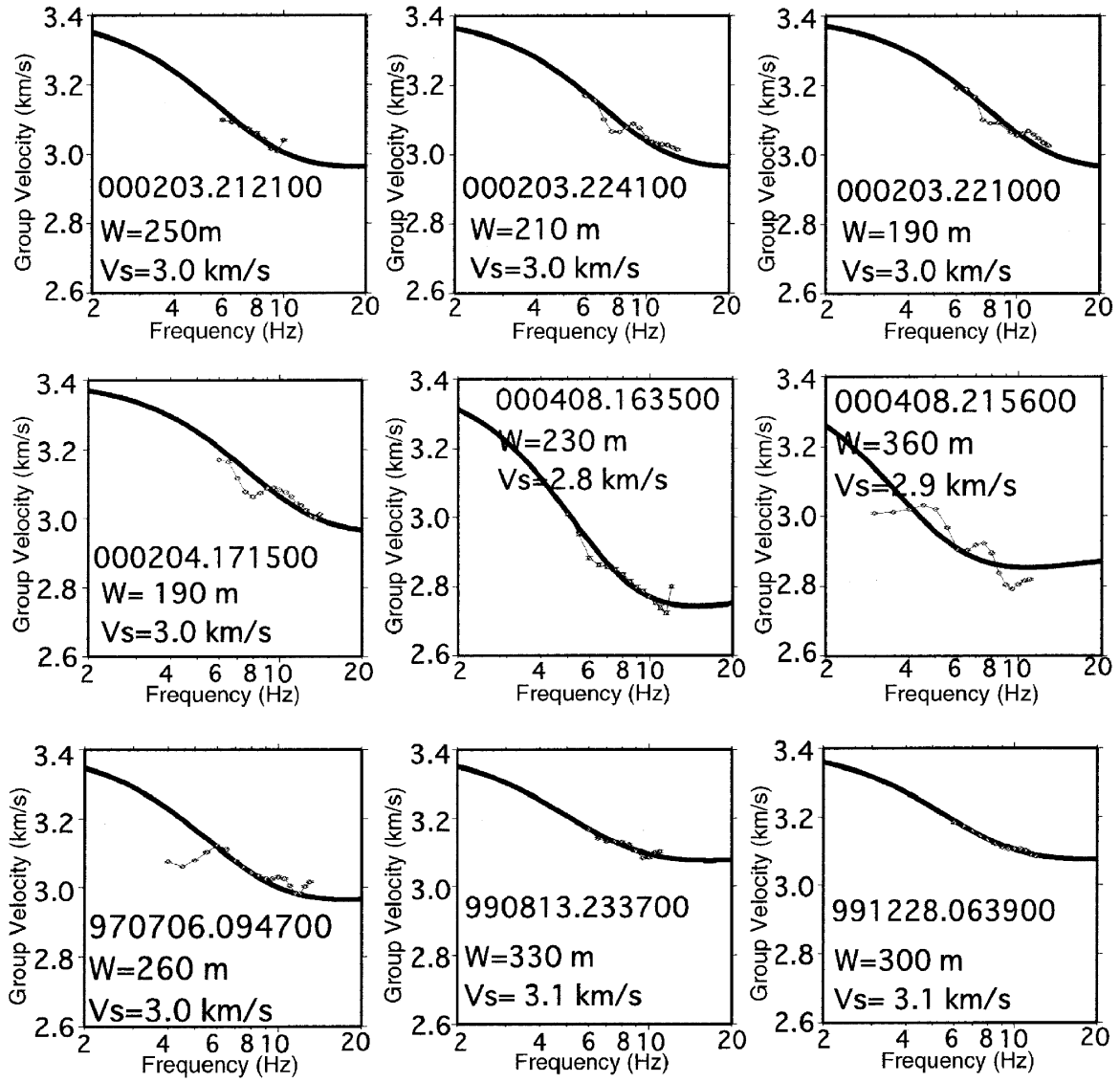


Fig. 10. Observation (thin line) and best-fit model (thick line) of the group velocity dispersion curve of the trapped waves.

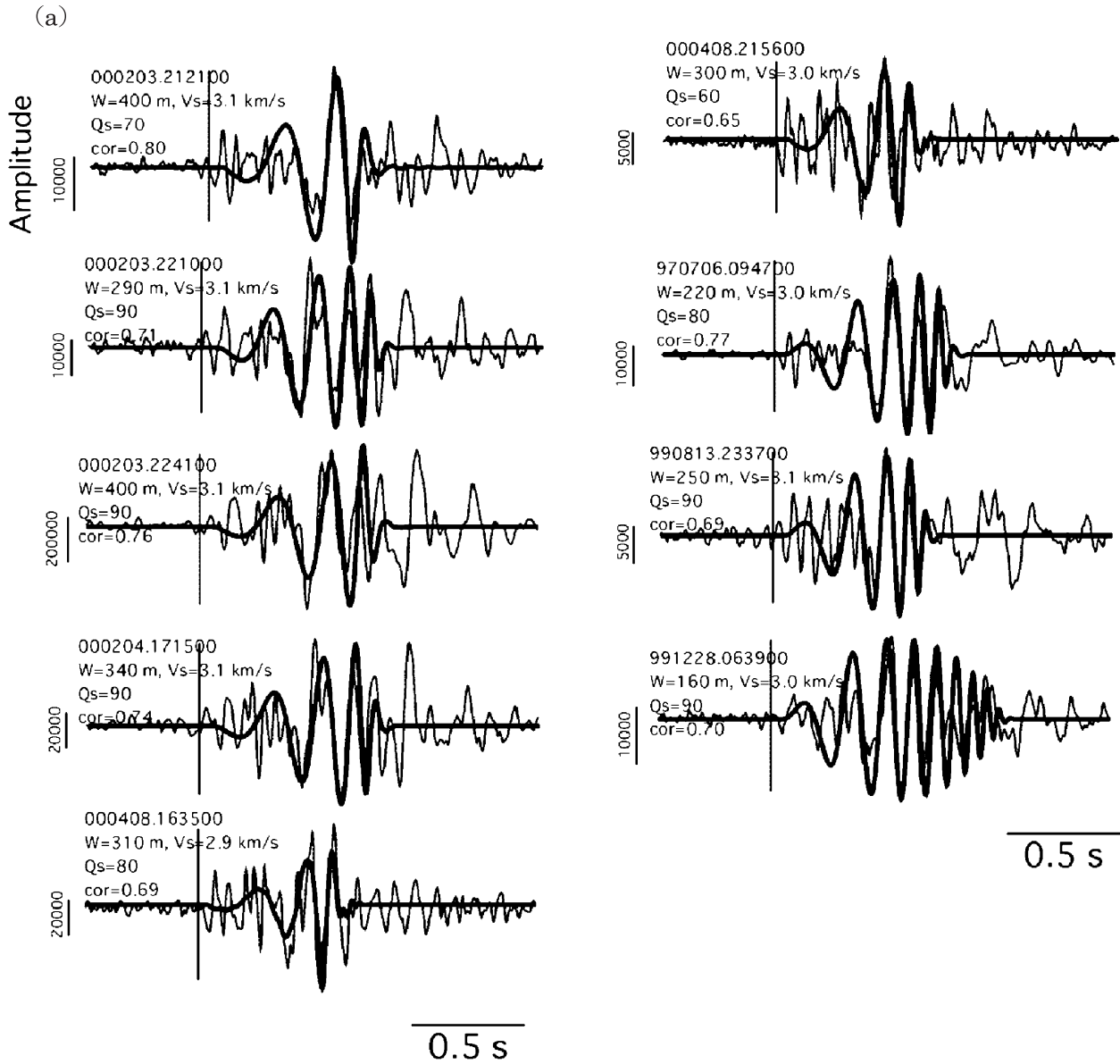


Fig. 11. Observation (thin line) and best-fit synthetic waveforms (thick line) for (a) mz08 and for (b) eight stations (mz03, mz08, mz11, mz15, mz19, mz23, mz27 and mz31). Model parameters for each model were also listed.

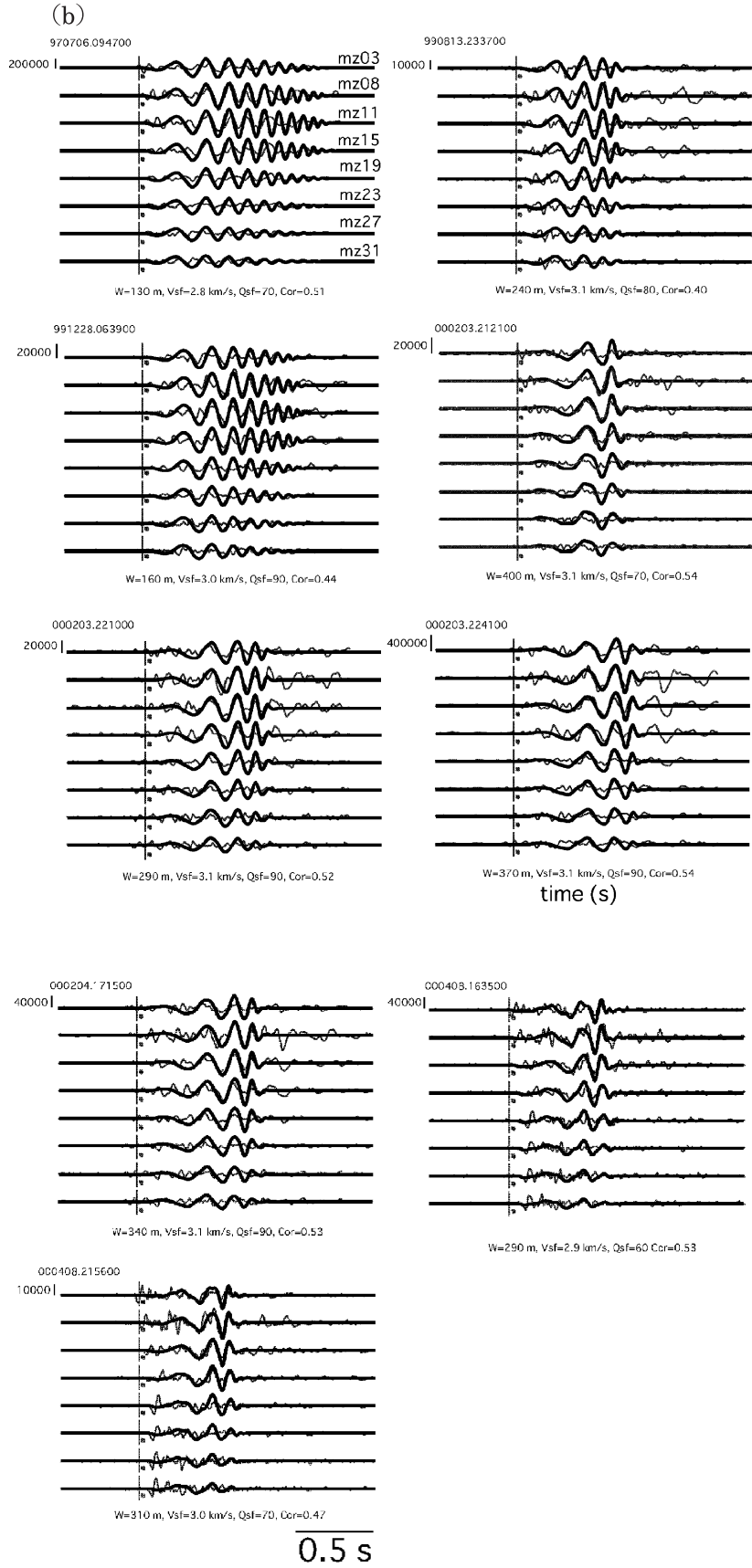


Fig. 11. (Continued.)

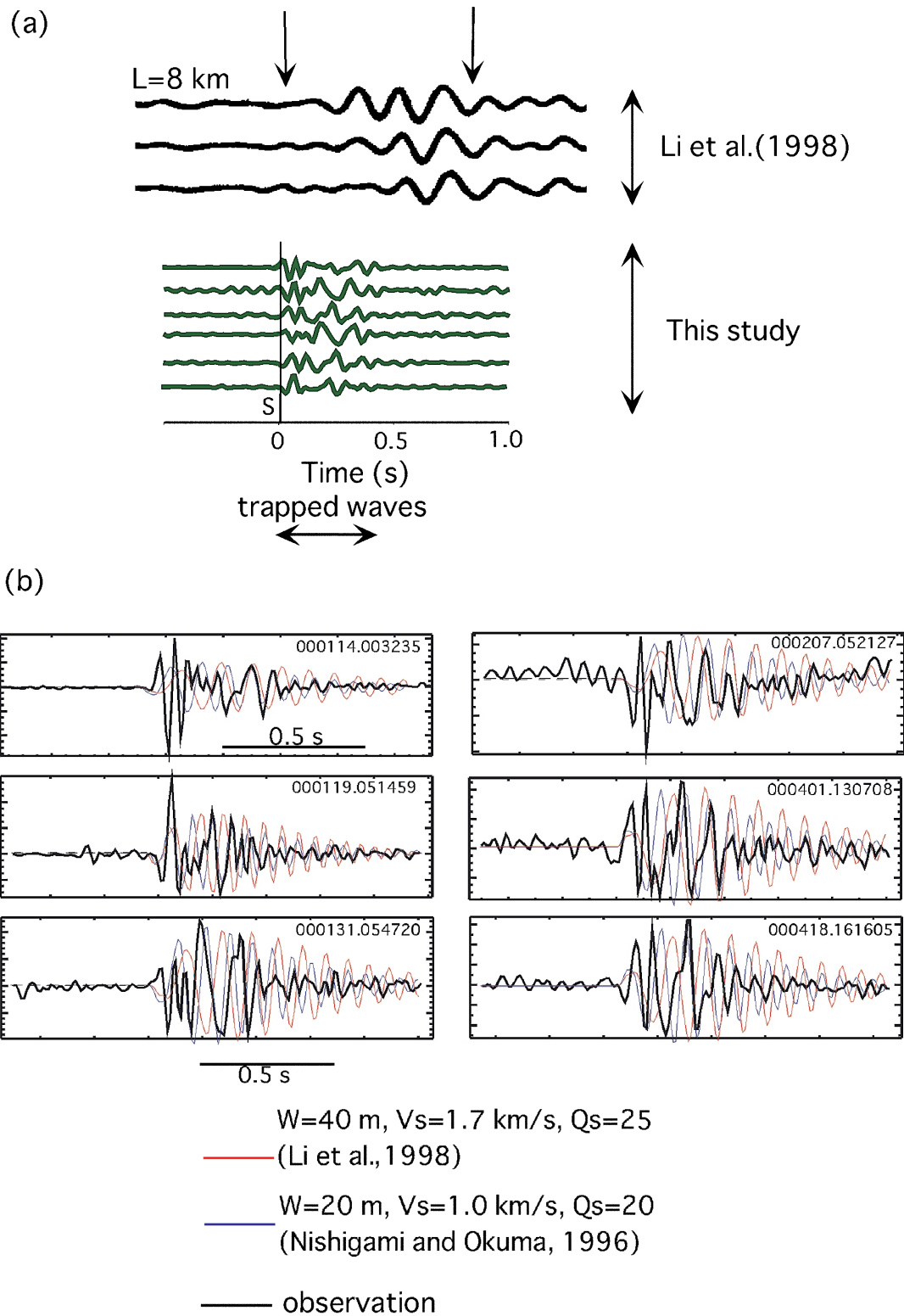


Fig. 12. (top) Examples of the trapped waves at the surface. The fault-parallel components of the seismograms at the Ezaki array operated by Li *et al.* (1998) are shown. The hypocentral distance was about 8 km. The shear-wave arrival is denoted by the first arrow in the plot. The second arrow denotes the duration of the fault-zone trapped waves. (Bottom) Typical trapped waves observed at borehole station, TOS2, in this study. (b) Comparisons between observed and synthetic waveforms expected from previous studies.

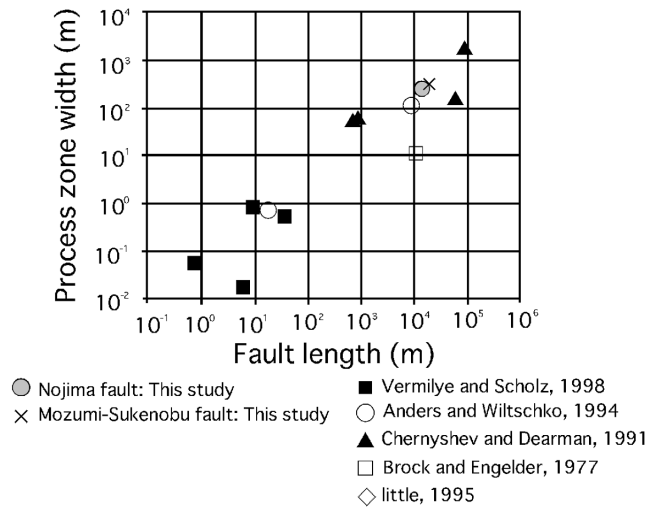


Fig. 13. Diagram showing the relation between the thickness of the fault-zone and the length of the fault (modified from Vermilye and Scholz, 1998).

of the circular crack. O'Connell and Budiansky (1974) predicted the relationship between ε and velocity reduction. If we assume that the fault zone was made by a fractured host rock (assuming no cracks within the host rock), we obtain a crack density ε of 0.5 for the shallower part (shallower than 4 km) and of 0.2 for the deep portion of the fault zone of the Nojima fault. Some studies infer the crack density and saturation rate in and around the active fault using tomographic data (e.g., Zhao and Mizuno, 1999). The detailed crack distribution in and around the fault can also be imaged by a combination of trapped waves and seismic tomography in the future.

5. Conclusion

Our conclusions are summarized below:

- (1) We observed typical fault-zone trapped waves using subsurface seismic observations at two active faults in Japan. The thickness and the shear-wave velocity of the fault zone was estimated by fitting observed and synthetic dispersion curves and waveforms. The best-fitting structure parameters are as follows: fault zone thickness is 150 m to 290 m for the Nojima fault, and 130 m to 400 m for the Mozumi-Sukenobu fault, shear-wave velocity is 10 to 20% less than the surrounding velocity.

- (2) At the Nojima fault, the width and the shear-wave velocity of the fault zone were larger than those of previous surface studies. We did not observe the wavetrain that was expected from the narrower fault model suggested by surface observations. Therefore, our model was preferable for explaining our observations. This discrepancy may be caused by spatial variations of the fault-zone structure and/or by observational conditions, such as a thick sedimentary layer near the surface. Borehole observations are preferable to conventional surface observations to detect trapped waves.

Acknowledgments

We are grateful to Drs. K. Nishigami at the Kyoto University, H. Ito and Y. Kuwahara at the Geological Survey of Japan, Y. Ben-Zion and Y.-G., Li at the University of Southern California for their helpful discussions on the analysis of trapped waves. Valuable comments by Dr. H. Ito at Geological Survey of Japan and R. Hino at Tohoku University are greatly appreciated.

References

- Ando, M., 1999. Overview and purpose of the active fault prove at the Mozumi-Atotsugawa fault system, *EOS Trans. AGU*, F739.

- Astrom, J. A., H. J. Herrmann and J. Timonen, 2000. Granular packings and fault zones, *Phys. Rev. Lett.*, **84**, 638–641.
- Baisch S., and G.H.R. Bokelmann, 2001. Seismic waveform attributes before and after the Loma Prieta earthquake : Scattering change near the earthquake and temporal recovery, *J. geophys. Res.*, **106**, 16323–16337.
- Ben-Zion, Y., and K. Aki, 1990. Seismic radiation from a SH line source in a laterally heterogeneous planer fault zone, *Bull. Seism. Soc. Am.*, **80**, 971–994.
- Ben-Zion, Y., 1998. Properties of seismic fault zone waves and their utility for imaging low-velocity structures, *J. geophys. Res.*, **103**, 12567–12585.
- Blenkinshop, T.G. 1989. Thickness-displacement relationships for deformation zones: Discussion. *J. Struct. Geol.*, **11**, 1051–1053.
- Byerlee, J.D., 1990. Friction, overpressure and fault normal compression, *Geophys. Res. Lett.*, **17**, 2109–2112.
- Byerlee, J.D., 1993. Model for episodic flow of high-pressure water in fault zones before earthquakes, *Geology*, **21**, 303–306.
- Chester F.M., J.P., Evans, and R.L., Biegel, 1993. Internal structure and weakening Mechanisms of the San Andreas fault, *J. geophys. Res.*, **98**, 771–786.
- Dresen, L., and H. Ruter, 1994. Seismic coal exploration, Part B: In-seam seismics, Handboob of geophysical exploration, Section 1, seismic exploration, Pergamon.
- Evans, J.P. 1990. Thickness-displacement relationships for fault zones, *J. Struct. Geol.* **12**, 1061–1065.
- Hashimoto, M., and D.D. Jackson, 1993. Plate tectonics and crustal deformation around the Japanese Islands, *J. geophys. Res.*, **98**, 16149–16166.
- Hole, J. A., T. M. Brocher, S. L. Klemperer, T. Parsons, H. M. Benz and K. P. Furlong, 2000. Three-dimensional seismic velocity structure of the San Francisco Bay area, *J. geophys. Res.*, **105**, 13859–13874.
- Hori, S., H. Inoue, Y. Fukao and M. Ukawa, 1985. Seismic detection of the untransformed 'basaltic' oceanic crust subducting into the mantle, *Geophys. J. R. astr. Soc.*, **83**, 169–197.
- Hudson, J. A., 1980. Wave speeds and attenuation of elastic waves in material containing cracks, *Geophys. J. R. astr. Soc.*, **64**, 133–150.
- Ito, H., and Y. Kuwahara, 2000. Deep structure of the Nojima fault by trapped wave analysis, Proc. The international workshop on the Nojima fault core and borehole data analysis, GSJ Interim Report, EQ/00/1, Geological Survey of Japan, Japan.
- Li, Y-G., K. Aki, J.E. Vidale and M.G. Alvarez, 1998. A delineation of the Nojima fault ruptured in the M7.2 Kobe, Japan, earthquake of 1995 using fault zone trapped waves, *J. geophys. Res.*, **103**, 7247–7263.
- Li, Y-G., J.E. Vidale, K. Aki and F. Xu, 2000. Depth-dependent structure of the Landers fault zone from trapped waves generated by aftershocks, *J. geophys. Res.*, **105**, 6237–6254.
- Maillois, B., S. Nielsen and I. Main, 1999. Numerical simulation of seismicity due to fluid injection in a brittle poroelastic medium, *Geophys. J. Int.*, **139**, 263–272.
- Mamada, Y., Y. Kuwahara and H. Ito, 2002. 3-D finite-difference simulation of seismic fault zone waves-Application to the fault zone structure of the Mozumi-Sukenobu fault, central Japan-, *Earth Planet and Space*, **54**, 1055–1058.
- Matsumoto, S., 2000. Temporal change in P-wave scatterer distribution associated with the M6.1 earthquake near Iwate volcano, northeastern Japan, *Geophys. J. Int.*, **145**, 48–58.
- Mizuno, T., and K. Nishigami, 2003. Deep structure of the Nojima Fault, Japan, estimated from a borehole observation of trapped waves, *Tectonophysics*. In preparation.
- Mizuno, T., K. Nishigami, H. Ito and Y. Kuwahara, 2003. Deep structure of the Mozumi-Sukenobu fault, central Japan, estimated from the subsurface array observation of fault zone trapped waves, *Geophys. J. Int.*, submitted.
- Mizuno, T., K. Yomogida, H. Ito and Y. Kuwahara, 2001. Spatial distribution of shear wave anisotropy in the crust of the southern Hyogo region by borehole observations, *Geophys. J. Int.*, **147**, 528–542.
- Murata, A., K. Takemura, T. Miyata and A. Lin, 2001. Quaternary vertical offset and average slip rate of the Nojima fault on Awaji Island, Japan, *The Island Arc*, **10**, 360–367.
- Nagai, S., Y. Kano, K. Tadokoro, T. Mizuno, H. Yamanaka, S. Ohmi, K. Nishigami, Y. Hiramatsu and N. Hirata, 2001. Microseismic observations during a water injection experiment in 2000 at the Nojima fault, Japan, *Bull. Earthq. Res. Inst. Univ. Tokyo.*, **76**, 163–186.
- Nishigami, K. and Y. Okuma, 1996. Crustal heterogeneity around the source region of the 1995 Kobe earthquake (M7.2): Deep structure of the Nojima fault and the scatterer distribution in the crust. EOS Transactions of the American Geophysical Union, **76**, F508.
- Nishigami, K., M. Ando and K. Tadokoro, 2001. Seismic observations in the DPRI 1800 m borehole drilled into the Nojima fault zone, south-west Japan, *The Island Arc*, **10**, 288–295.
- O'Connell, R. J., and B. Budiansky, 1974. Seismic velocities in dry and saturated cracked solid, *J. geophys. Res.*, **79**, 5412–5426.
- Ohtani, T., H. Tanaka, K. Fujimoto, T. Higuchi, N. Tomida and H. Ito, 2001. Internal structure of the Nojima fault zone from Hirabayashi GSJ drill core, *The Island Arc*, **10**, 392–400.
- Park, J.-O., T. Tsuru, S. Kodaira, A. Nakanishi, S. Miura, Y. Kaneda and Y. Kono, 2000. Out-of-sequence thrust faults developed in the coseismic slip zone of the 1946 Nankai earthquake (Mw=8.2) off Shikoku, Southwest Japan, *Geophys. Res. Lett.*, **27**, 1033–1036.
- Rader, D., W. Schott, L. Dresen and H. Ruter, 1985. Calculation of dispersion curves and amplitude-depth distributions of Love channel waves in horizontally-layered media, *Geophys. Prospect.*, **33**, 800–816.
- Reguero, J., 1990. Seam waves: What are they used for?, *The Leading Edge*, **9**, 19–23.
- Sagiya, T., S. Miyazaki and T. Tada, 2000. Continuous GPS array and present-day crustal deformation of Japan, *PAGEOPH*, **157**, 2303–2322.
- Shipton, Z. K., and P. A. Cowie, 2001. Damage zone and slip-surface evolution over micro meter to kilo meter scales in high-porosity Navajo sandstone, Utah, *J. struct. Geol.*, **23**, 1825–1844.

- Scholz, C.H., N.H. Dawers, J. -Z. Yu and M.H. Anders, 1993. Fault growth and fault scaling laws: preliminary results, *J. geophys. Res.*, **98**, 21591–21961.
- Sibson, R.H., 1992. Implications of fault-valve behavior for rupture nucleation and recurrence, *Tectonophysics*, **211**, 283–293.
- Tadokoro, K., and M. Ando, 2002. Evidence for rapid fault healing derived from temporal changes in S wave splitting, *Geophys. Res. Lett.*, **29**, 10.1029/2001GL013644.
- Takeuchi, A., H. Ongirad, A. Takebe, K. Sakogaichi and T. Nohara, 1999. Results of excavation survey on the Mozumi-Sukenobu fault of the Atotsugawa fault system, Central Japan. American Geophysical Union 1999 Fall Meeting, S51A-23.
- Tanaka, H., K. Fujimoto, T. Ohtani and H. Ito 2001. Structural and chemical characterization of shear zones in the freshly activated Nojima fault, Awaji Island, southwest Japan, *J. geophys. Res.*, **106**, 8789–8810.
- The research group for active faults in Japan, 1991. Active faults in Japan-sheet maps and inventories-, Univ. of Tokyo Press, pp. 437 (in Japanese).
- Thurber, C., S. Roecker, W. Ellsworth, Y. Chen, W. Lutter and R. Sessions, 1997. Two-dimensional seismic image of the San Andreas fault in the Northern Gabilan range, Central California: Evidence for fluids in the fault zone. *Geophys. Res. Lett.*, **24**, 1591–1594.
- Vermilye, J.M., and C.H. Scholz, 1998. The process zone: micro-structural view of fault growth, *J. geophys. Res.*, **103**, 12223–12237.
- Yamashita, T., 1998. Simulation of seismicity due to fluid migration in a fault zone, *Geophys. J. Int.*, **132**, 674–686.
- Zhang, A., F.C. Wagner, S. Stanchits, C. Janssen and G. Dresen, 2000. Fracture process zone in granite, *J. geophys. Res.*, **105**, 23651–23661.
- Zhao, D., and T. Mizuno, 1999. Crack density and saturation rate in the 1995 Kobe earthquake region, *Geophys. Res. Lett.*, **26**, 3213–3216, 1999.
- Zhao, D., and H. Negishi, 1998. The 1995 Kobe earthquake: seismic image of the source zone and its implications for the rupture nucleation, *J. geophys. Res.*, **103**, 9967–9986.

(Received December 17, 2002)
(Accepted May 7, 2003)